Atmos. Chem. Phys. Discuss., doi:10.5194/acp-2016-412, 2016
Manuscript under review for journal Atmos. Chem. Phys.
Published: 1 June 2016

Atmospheric Chemistry and Physics Discussions

Impacts of heterogeneous uptake of dinitrogen pentoxide and chlorine activation on ozone and reactive nitrogen partitioning: Improvement and application of WRF-Chem model in southern China

Qinyi LI[1], Li ZHANG[1], Tao WANG[1]*, Yee Jun THAM[1], Ravan AHMADOV[2,3], Likun XUE[4], Qiang ZHANG[5], and Junyu ZHENG[6]

[1] Department of Civil and Environmental Engineering, The Hong Kong Polytechnic University, Hong Kong, China,
[2] Cooperative Institute for Research in Environmental Sciences, University of Colorado at Boulder, Boulder, CO, USA,
[3] Earth System Research Laboratory, National Oceanic and Atmospheric Administration, Boulder, CO, USA,
[4] Environment Research Institute, Shandong University, Ji'nan, China,
[5] Center for Earth System Science, Tsinghua University, Beijing, China,
[6] School of Environmental Science and Engineering, South China University of Technology, Guangzhou, China.

* *Correspondence to:* T. Wang (cetwang@polyu.edu.hk)

Abstract: The uptake of dinitrogen pentoxide (N_2O_5) on aerosol surfaces and the subsequent production of nitryl chloride ($ClNO_2$) can have significant impact on the oxidising capability and thus on secondary pollutants such as ozone. The range of such impact, however, has not well been quantified in different geographical regions. In this study, we applied Weather Research and Forecasting coupled with Chemistry (WRF-Chem) model to investigate the impact of the N_2O_5 uptake processes in the Hong Kong-Pearl River Delta (HK-PRD) region, where the highest ever-reported N_2O_5 and $ClNO_2$ concentrations were observed in our recent field study. We first incorporated into the WRF-Chem an aerosol thermodynamics model (ISORROPIA II), recent parameterisations for N_2O_5 heterogeneous uptake and $ClNO_2$ production and gas-phase chlorine chemistry. The revised model was then used to simulate the spatiotemporal distribution of N_2O_5 and $ClNO_2$ over the HK-PRD region and the impact of N_2O_5 uptake and Cl activation on ozone and reactive nitrogen in the planetary boundary layer (PBL). The updated model is capable of reproducing the temporal patterns of N_2O_5 and $ClNO_2$ observed at a mountain-top site in Hong Kong, but overestimates N_2O_5 uptake and $ClNO_2$ production. The model results suggest that under average meteorological conditions, elevated levels of $ClNO_2$ (>0.25 ppb within the PBL) are present in the south-western PRD, with the highest values (>1.00 ppb) predicted near the ground surface (0-200 m above ground level (a.g.l.)). In contrast, during the night when very high levels of $ClNO_2$ and N_2O_5 were measured in well-processed plumes from the PRD, $ClNO_2$ is mostly concentrated within the residual layer (~300 m a.g.l.). The addition of N_2O_5 heterogeneous uptake and Cl activation reduces the NO and NO_2 levels by as much as 1.93 ppb (~7.4%) and 4.73 ppb (~16.2%), respectively, increases the total nitrate and ozone concentrations by up to 13.45 μg m^{-3} (~ 57.4%) and 7.23 ppb (~16.3%), respectively, in the PBL. Sensitivity tests show that the simulated chloride and $ClNO_2$ concentrations are highly sensitive to chlorine emission. Our study suggests the need to measure the vertical profiles of N_2O_5/$ClNO_2$ under various meteorological conditions, to consider the chemistry of N_2O_5/$ClNO_2$ in the chemical transport model, and to develop an updated chlorine emission inventory over China.

Atmos. Chem. Phys. Discuss., doi:10.5194/acp-2016-412, 2016
Manuscript under review for journal Atmos. Chem. Phys.
Published: 1 June 2016

Atmospheric Chemistry and Physics Discussions

1 Introduction

Dinitrogen pentoxide (N_2O_5) is mostly produced by chemical reactions involving ozone (O_3) and nitrogen dioxide (NO_2).

$$O_3 + NO_2 \longrightarrow NO_3 \qquad (1)$$

$$NO_3 + NO_2 \longrightarrow N_2O_5 \qquad (2)$$

The subsequent heterogeneous uptake of N_2O_5 produces nitrate on water-containing aerosol surfaces via reaction 3 (hydrolysis) and produces both nitrate and gaseous nitryl chloride ($ClNO_2$) on chloride-containing aerosol surfaces via reaction 4 (Finlayson-Pitts et al., 1989; Osthoff et al., 2008). The net reaction of reactions 3 and 4 could be treated as reaction 5, in which the $ClNO_2$ yield, i.e. parameter ϕ, represents the fraction of N_2O_5 that reacts via reaction 4. The produced $ClNO_2$ can be further photolysed into Cl radical and NO_2 (via reaction 6).

$$N_2O_5(g) + H_2O(aq) \longrightarrow 2\ HNO_3(aq) \qquad (3)$$

$$N_2O_5(g) + HCl(aq) \longrightarrow HNO_3(aq) + ClNO_2(g) \qquad (4)$$

$$N_2O_5(g) + (1\text{-}\phi)H_2O(aq) + \phi\ HCl(aq) \longrightarrow (1\text{-}\phi)\times 2\ HNO_3(aq) + \phi\times(HNO_3(aq) + ClNO_2(g)) \qquad (5)$$

$$ClNO_2(g) + h\nu \longrightarrow Cl\ (g) + NO_2(g) \qquad (6)$$

The above processes affect the fate and composition of the total reactive nitrogen (NO_y), which is the sum of NO, NO_2, HNO_3 (g), $2*N_2O_5$, NO_3, $ClNO_2$, PAN, HONO, HNO_4, aerosol nitrate, and various organic nitrates. The hydrolysis of N_2O_5 is the major loss pathway for NO_x (=NO+NO_2) at night, reducing the amount of NO_x for daytime photochemistry in the following day, while producing nitrate aerosol contributing to secondary aerosol (Brown and Stutz, 2012). When $ClNO_2$ is produced, it serves as a reservoir for reactive nitrogen at night and is photolysed to recycle NO_2 and release highly reactive chlorine radicals (Cl activation), both of which can significantly affect the daytime photochemistry, such as O_3 formation via reactions with volatile organic compounds (VOCs) (Atkinson, 2000; Thornton et al., 2010; Riedel et al., 2014).

The critical parameters required to determine the impacts of the N_2O_5 uptake processes are the rate constant of reaction 5, k_5, and the yield of $ClNO_2$, ϕ. k_5 can be calculated from Eq. (1) by treating the N_2O_5 heterogeneous uptake reaction as a first order reaction (Chang et al., 2011),

$$k_5 = \frac{V_{N_2O_5} \times S_{aer} \times \gamma}{4}, \qquad \text{(Equation 1)}$$

where $V_{N_2O_5}$ denotes the mean molecular velocity of N_2O_5, S_{aer} is the aerosol surface to volume ratio, and γ represents the heterogeneous uptake coefficient of N_2O_5. $V_{N_2O_5}$ and S_{aer} are relatively well determined; therefore, the treatments of γ and ϕ are crucial for the prediction of the impacts of N_2O_5 uptake and Cl activation. In terms of γ, a fixed value of 0.1 was first proposed (Dentener and Crutzen, 1993). Later studies considered dependence of γ on the aerosol species/compositions (sea

Atmos. Chem. Phys. Discuss., doi:10.5194/acp-2016-412, 2016
Manuscript under review for journal Atmos. Chem. Phys.
Published: 1 June 2016

Atmospheric Chemistry and Physics Discussions

salt, black carbon, sulfate, nitrate, chloride, organic matter and water), temperature and/or relative humidity (Evans and Jacob, 2005 and the reference therein; Davis et al., 2008; Anttila et al., 2006; Riemer et al., 2009; Bertram and Thornton, 2009). Several parameterisations have been proposed for the yield of $ClNO_2$. Simon et al. (2010) applied a constant value of 0.75 for the fraction of N_2O_5 involved in the production of $ClNO_2$. More detailed parameterisations of ϕ considering the effects of aerosol compositions were proposed by Roberts et al. (2009) and by Bertram and Thornton (2009).

Several studies have been conducted to examine the impacts of N_2O_5 uptake *or* $ClNO_2$ production with the use of the chemical transport model. Lowe et al. (2015) and Archer-Nicholls et al. (2014) incorporated the heterogeneous uptake of N_2O_5 on particles into the MOSAIC aerosol module in WRF-Chem based on the methods suggested by Bertram and Thornton (2009), Anttila et al. (2006) and Riemer et al. (2009). Their results suggested that N_2O_5 uptake suppressed VOC oxidation (by OH and NO_3) by a factor of 1.5 and significantly enhanced nitrate formation during nighttime (an increase from 3.5 to 4.6 μg Kg^{-1}) over north-western Europe. Sarwar et al. (2012) implemented the heterogeneous production of $ClNO_2$ based on the parameterisation proposed by Bertram and Thornton (2009) and additional gas-phase chlorine reactions in CMAQ and examined the impacts of Cl activation due to $ClNO_2$ production and Cl chemistry on air quality. Their results showed that $ClNO_2$ production reduced the total nitrate level (up to 0.8-2.0 μg m^{-3} or 11-21%) and had modest impacts on the 8-h O_3 level (up to 1-2 ppb or 3-4%) in the United States. Sarwar et al. (2014) expanded the study region used in Sarwar et al. (2012) to the entire northern hemisphere and suggested that $ClNO_2$ production had remarkable impacts on the air quality in China and western Europe with enhancements of the 8-h O_3 level up to 7.0 ppb. Most previous studies focused on investigating the effects of N_2O_5 uptake or $ClNO_2$ production in North America and Europe; however, little is known about Asia. The only study that covered Asia was performed by Sarwar et al. (2014); it used a coarse model resolution (>100 Km) and considered only biomass burning as the source of chloride over land.

Previous studies in Asia (Hong Kong) have revealed the existence and significance of $ClNO_2$ in this region (Wang et al., 2014; Tham et al., 2014; Xue et al., 2015). In a recent field study, we observed the highest ever-reported mixing ratios of N_2O_5 (1-minute value up to 7.7 ppbv) and $ClNO_2$ (4.7 ppbv) at a mountain top site (957m above sea level) in Hong Kong (Brown et al., 2016; Wang et al., 2016). This result indicates rapid production of N_2O_5 and $ClNO_2$ in the Hong Kong-Pearl River delta (HK-PRD) region which has long suffered O_3 and NO_x pollution (Wang et al., 2009). Meteorological analysis and chemical data revealed highly inhomogeneous dynamic and chemical processes and considerable impacts of the $ClNO_2$ chemistry on the radical budget (up to 77% increase of OH) and daytime O_3 production (up to 41%) in the high $ClNO_2$ air mass as it transported to downwind locations above the ocean (Wang et al., 2016). It was also suggested in that study that other locations downwind of major urban areas under prevailing conditions may experience more frequent events with high levels of $ClNO_2/N_2O_5$ than the site in Hong Kong. It is therefore of great interest to investigate the regional distribution of $N_2O_5/ClNO_2$ and the impact of N_2O_5 uptake and subsequent chemistry.

Atmos. Chem. Phys. Discuss., doi:10.5194/acp-2016-412, 2016
Manuscript under review for journal Atmos. Chem. Phys.
Published: 1 June 2016

Atmospheric Chemistry and Physics Discussions

This study was conducted to investigate (1) the spatial (horizontal and vertical) distribution of the N_2O_5 and $ClNO_2$ concentrations in the HK-PRD region and (2) the spatial extent of the impact of N_2O_5 uptake processes on the formation of O_3 and the partitioning of reactive nitrogen in this region. The latest version of a widely used aerosol thermodynamics model, ISORROPIA II (Fountoukis and Nenes, 2007), was incorporated into the MADE/VBS aerosol model. ISORROPIA II has the ability to simulate the equilibrium between hydrogen chloride (HCl) and chloride which is critical for the simulation of N_2O_5 heterogeneous uptake and Cl activation. But this capacity is not considered in the current MADE/VBS model in WRF-Chem (Grell et al., 2005; Ahmadov et al., 2012). Up-to-date parameterisation for N_2O_5 uptake and $ClNO_2$ production and Cl radical initiated chemistry were implemented into WRF-Chem. The revised WRF-Chem was then applied to southern China to investigate the spatial distribution of N_2O_5 and $ClNO_2$ and the impacts of these processes on O_3 and NO_y. We start with a description of the data used to run and validate the simulations, the amendments to the WRF-Chem model, and the model setup in Section 2. In Section 3, we show the performance of the WRF-Chem model in the simulation of several air pollutants without N_2O_5 uptake processes, and the simulation results of N_2O_5 and $ClNO_2$ with N_2O_5 uptake and Cl activation processes; we then evaluate the impacts of N_2O_5 uptake and Cl activation on NO_x, total nitrate, O_3 and NO_y partitioning, and test the sensitivity of the $ClNO_2$ concentration to chlorine emissions. A summary is given in Section 4.

2 Methodology

2.1 Data

2.1.1 Field measurement data

N_2O_5 and $ClNO_2$ concentrations were measured at Tai Mo Shan (TMS) in Hong Kong with a chemical ionization mass spectrometer between November 15 and December 5, 2013 (refer to Wang et al., 2016 for more details). The measurements were made on a mountain top in the south-eastern PRD at an altitude of 957m. Other major air pollutants, including $PM_{2.5}$, NO_2, and O_3, were also measured at the TMS site and at 11 general (non-roadside) monitoring stations of the Hong Kong Environmental Protection Department (HKEPD; available at: http://epic.epd.gov.hk/EPICDI/air/station/). Hourly measurement data were used to validate the performance of the WRF-Chem simulations.

2.1.2 Emission data

Four sets of anthropogenic emission inventories (EIs) covering different areas were adopted in this study. For mainland China, we used the Multi-resolution Emission Inventory for China (MEIC; available at http://meicmodel.org), developed by Tsinghua University for year 2010. For the PRD, the anthropogenic EI developed by the Southern China University of Technology was applied. The anthropogenic EI developed by HKEPD was used over Hong Kong. INTEX-B EI (Zhang et al., 2009) was adopted for other Asian regions. Readers are referred to Zhang et al. (2016) for the details of these anthropogenic EIs. For natural

Atmos. Chem. Phys. Discuss., doi:10.5194/acp-2016-412, 2016
Manuscript under review for journal Atmos. Chem. Phys.
Published: 1 June 2016

emissions, the biogenic emission parameterisation proposed by Guenther et al. (1994), the dust emission parameterisation proposed by Shaw et al. (2008) and the sea salt emission parameterisation proposed by Gong et al. (2002) were adopted in this study. The concentrations of sodium, chloride, calcium, magnesium and potassium in dust and sea salt follow those suggested by Millero (1996) and Wedepohl (1995), as shown in Table S1.

Chlorine emissions are not included in most EIs, but they are critical for the simulation of N_2O_5 uptake and Cl activation. In this study, the Reactive Chlorine Emission Inventory (RCEI) (Keene et al., 1999 and references therein, available at http://eccad.sedoo.fr/eccad_extract_interface/JSF/page_login.jsf) with a resolution of 1°x1° was adopted to provide chlorine emissions, including emissions from biomass burning and anthropogenic activities (e.g. coal combustion). Global chlorine emissions from biomass burning and anthropogenic activities are estimated to be ~6.3 Tg Cl yr^{-1} and ~6.6 Tg Cl yr^{-1}, respectively. The RCEI inventory is the only available chlorine EI that currently covers China, and it is subject to some, probably large, uncertainties for representing Cl emissions in the HK-PRD region due to its low spatial resolution and the fact that it was compiled for year 1990. Coal consumption and SO_2 emissions from coal-fired power plants in China increased by 479% and 56% from 1990 to 2010, respectively (Liu et al., 2015); thus it is expected that chlorine emissions from coal combustion, which form a large proportion of anthropogenic chlorine (Keene et al., 1999), also increased significantly over that period. We conducted two sensitivity simulations by adjusting the chlorine emissions to test the dependence of the chloride and $ClNO_2$ concentrations on the varied chlorine emissions; the results are shown in Section 3.5.

2.1.3 Meteorological data

Three-hourly meteorological measurements, including atmospheric pressure, temperature, relative humidity, wind direction and wind speed, at ~2500 surface meteorological stations and twelve-hourly data at ~250 sounding stations, were obtained from the China Meteorological Agency (CMA) and Hong Kong Observatory and were adopted in Four-Dimensional Data Assimilation to improve the model performance of the meteorological fields using observational nudging techniques (Zhang et al., 2016). The FNL Operational Global Analysis dataset provided by the National Centers for Environmental Prediction (available at http://rda.ucar.edu/datasets/ds083.2/) was used for analysis nudging. Observational and analytical nudging techniques have been shown to improve the performance of meteorological simulation in both northern China (Zhang et al, 2015) and southern China (Zhang et al., 2016). Hourly datasets from ~500 surface meteorological observation stations obtained from the CMA were used to validate the meteorological simulations.

2.2 Model development

2.2.1 Incorporation of ISORROPIA II

ISORROPIA II, an aerosol thermodynamics model developed by Nenes et al. (1998) and Fountoukis and Nenes (2007), was incorporated to replace the aerosol thermodynamics module in the MADE/VBS aerosol model in the original WRF-Chem v3.5

Atmos. Chem. Phys. Discuss., doi:10.5194/acp-2016-412, 2016
Manuscript under review for journal Atmos. Chem. Phys.
Published: 1 June 2016

Atmospheric Chemistry and Physics Discussions

so as to extend the capacity of simulation of the equilibrium between $PM_{2.5}$ compositions and their corresponding gaseous species. The MADE/VBS model adopts volatility basis set model to simulate secondary organic aerosol (SOA) formation and provides improved simulations of SOA compared to the traditional MADE/SORGAM model (Ahmadov et al., 2012). The current MADE/VBS model only estimates the thermodynamic equilibrium between SO_4^{2-}, NO_3^-, NH_4^+, H_2O and corresponding gases, whereas ISORROPIA II simulates the equilibrium between SO_4^{2-}, NO_3^-, NH_4^+, H_2O, Na^+, Cl^-, Ca^{2+}, Mg^{2+}, K^+ and associated gases.

2.2.2 N_2O_5 heterogeneous uptake, $ClNO_2$ production and Cl gaseous reaction

We adopted the parameterisations of N_2O_5 heterogeneous uptake and $ClNO_2$ production suggested by Bertram and Thornton (2009). According to the parameterisations, the N_2O_5 heterogeneous uptake coefficient, γ, can be calculated with the following equation:

$$\gamma = Ak\left(1 - \frac{1}{\left(\frac{0.06[H_2O(l)]}{[NO_3^-]}\right)+1+\left(\frac{29[Cl^-]}{[NO_3^-]}\right)}\right) \qquad \text{(Equation 2)}$$

where $A=3.2\times10^{-8}$, $k=1.15\times10^{6}\times(1-e^{(-0.13[H_2O(l)])})$, and $[H_2O(1)]$, $[NO_3^-]$ and $[Cl^-]$ are the molarities of liquid water, nitrate, and chloride in aerosol volume. The yield of $ClNO_2$, ϕ, can be calculated with the following equation:

$$\phi = \left(1+\frac{[H_2O(l)]}{483[Cl^-]}\right)^{-1} \qquad \text{(Equation 3).}$$

The loss of N_2O_5 and the production of nitrate and $ClNO_2$ can be predicted with Eq. (1-3). The produced $ClNO_2$ is then photolysed, releasing a Cl atom, which further oxidises VOCs like an OH radical. The Cl-initiated gaseous chemistry used in this study was originally designed for CB05 mechanism by Sarwar et al. (2012), and was modified for RACM_ESRL mechanism (detail reactions are shown in Table S2). RACM_ESRL mechanism is the updated Regional Atmospheric Chemistry Mechanism in WRF-Chem based on the original version in Stockwell et al. (1997). The photolysis rates of Cl_2, HOCl, $ClNO_2$ and formyl chloride (FMCl) were calculated with the absorption cross section and quantum yield obtained from Atkinson et al. (2007) and Atkinson et al. (2008).

We implemented the N_2O_5 heterogeneous uptake, the $ClNO_2$ production, and the Cl-initiated reactions into the MADE/VBS aerosol model, RACM_ESRL gas-phase mechanism and Madronich photolysis model (Madronich, 1987) in the 'RACM_SOA_VBS_KPP' chemistry option in WRF-Chem v3.5.

2.3 Model setup

2.3.1 Model configuration

The model configurations of WRF-Chem used in this study are shown in Table 1. We used the Noah model to simulate the land surface process, the YSU module to simulate the PBL processes, the Purdue Lin scheme to predict the microphysics, the

Atmos. Chem. Phys. Discuss., doi:10.5194/acp-2016-412, 2016
Manuscript under review for journal Atmos. Chem. Phys.
Published: 1 June 2016

Grell 3-D ensemble module to simulate cumulus, the RRTMG model to predict shortwave and longwave radiation and the RACM_ESRL, MADE/VBS and Madronich modules to simulate gas-phase chemistry, aerosol processes and photolysis.

Model simulations were conducted in 4 domains covering East Asia, southern China, the PRD and Hong Kong, with spatial resolutions of 27, 9, 3, and 1 km, respectively (see Fig. 1a). High grid resolutions were adopted in this study to capture the extremely inhomogeneous terrain, with land and sea, mountain and plain, urban and forested areas, as shown in the terrain map of domain 2 (southern China) in Fig. 1b. The red dotted line in Fig. 1b represents the vertical cross-section domain that intercepts the most polluted part of the PRD and follows the prevailing (north-east) wind direction. The vertical domain is used to illustrate the vertical distribution of the N_2O_5 and $ClNO_2$ concentrations and the impacts of N_2O_5 uptake processes in southern China.

2.3.2 Simulation cases

Three simulation cases, shown in Table 2, were conducted from November 15 to December 5, 2013, during which $ClNO_2$ and N_2O_5 levels were measured at the TMS site. All simulations used ISORROPIA II as the aerosol thermodynamics module. Note that the Base case did not include N_2O_5 heterogeneous uptake (or $ClNO_2$ chemistry). The HET+Cl case included the complete N_2O_5 uptake and Cl activation processes, i.e., N_2O_5 loss on aerosol, $ClNO_2$ production and gaseous chlorine reactions. Differences in chemical concentrations between the Base and HET+Cl cases, i.e., HET+Cl-Base, represent the impacts of N_2O_5 uptake and Cl activation. To estimate the relative contribution of N_2O_5 uptake versus Cl activation to O_3 and NO_y partitioning, the HET case was also conducted, which included N_2O_5 uptake but not $ClNO_2$ production (i.e. $ClNO_2$ yield, ϕ, was set to 0) and therefore producing only nitrate from N_2O_5 uptake. The changes from the Base case to the HET case (HET-Base) represent the impacts of N_2O_5 heterogeneous uptake, whereas the changes from the HET case to the HET+Cl case (HET+Cl-HET), represent the impacts of Cl activation.

3 Results and discussion

3.1 Model performance of WRF-Chem without N_2O_5 uptake and Cl activation

The meteorological simulation determines the simulations of the transport of the air pollutants and therefore is crucial to the simulations of the spatial distributions of the atmospheric chemical species and their impacts. The performance of the meteorological module during the study period has been validated in Wang et al. (2016), which showed that atmospheric flow and other meteorological parameters were satisfactorily simulated. The reader is referred to Wang et al. (2016) for further details.

The chemical simulation results of WRF-Chem without N_2O_5 heterogeneous uptake and Cl activation, i.e., the Base case, were validated against hourly observations of several major air pollutants measured at 11 HKEPD stations and at the TMS site. $PM_{2.5}$, NO_2 and O_3 were selected as the validation species because they act as the reaction surface ($PM_{2.5}$) or precursors (NO_2

Atmos. Chem. Phys. Discuss., doi:10.5194/acp-2016-412, 2016
Manuscript under review for journal Atmos. Chem. Phys.
Published: 1 June 2016

Atmospheric Chemistry and Physics Discussions

and O_3) for N_2O_5 and $ClNO_2$ production. As shown in Table 3, the validation results for HKEPD stations indicate that Base case simulated the major air pollutants reasonably well in this region but overestimated $PM_{2.5,}$ slightly underestimated NO_2 and underestimated O_3. It should be noted that the technique for measuring NO_2 by the HKEPD, which is similar to that used in the regular air monitoring networks in North America and Europe, employs catalytic conversion which over-measures NO_2 (e.g., Xu et al., 2013). The discrepancy between the simulated and observed major air pollutants in this area is expected to affect the simulations of N_2O_5 and $ClNO_2$, which will be discussed in Section 3.2.1. In the Base case, the model, in general, satisfactorily reproduced the observed $PM_{2.5,}$ NO_2 and O_3 levels at the TMS site during the nights when N_2O_5 and $ClNO_2$ were measured (Fig. S1). The capture of the temporal variations of these pollutants at the TMS site provides a good basis for simulation of the N_2O_5 and $ClNO_2$ temporal patterns (see Section 3.2.1). The model performance of major air pollutants of Base case is within the acceptable range and is similar to our previous applications of WRF-Chem (Zhang et al., 2015; Zhang et al., 2016) and other WRF-Chem model studies (e.g., Li et al., 2011).

The simulated fine chloride concentrations in the Base case were compared with observations from several campaigns, as shown in Table 4. Tan et al. (2009) reported average concentrations of 1.19 μg m^{-3} and 8.37 μg m^{-3} at an urban site in Guangzhou (GZ) in the PRD on normal days and hazy days in winter, respectively; in comparison, the Base case simulated an average level of 2.51 μg m^{-3} at that location. Tao et al. (2014) reported an average level of 3.30 μg m^{-3} in winter at the station of South China Institute of Environmental Science (SCIES) in Guangzhou; Base case predicted 2.13 μg m^{-3} at this location. At the Tung Chung (TC) site in Hong Kong, we had previously measured an average level of 1.10 μg m^{-3} of chloride in $PM_{2.5}$ in late autumn and early winter, while the Base case simulated 0.32 μg m^{-3}. At the TMS site, an average level 0.37 μg m^{-3} of chloride was observed during the campaign (which was also the simulation period of this study), while the Base case predicted 0.14 μg m^{-3}. The simulated chloride level in the Base case was in order with observations over the PRD, but it still under-simulated the observed chloride level due to the expected underestimates of chlorine sources in the EI we applied (see Section 2.1.2).

Overall, the validations of the meteorological and chemical simulations suggest that the model is capable of capturing the general characteristics of air flow and key atmospheric chemical processes and hence can provide a basis for further simulation of the distributions of the N_2O_5 and $ClNO_2$ concentrations, and the impacts of N_2O_5 uptake and Cl activation on NO_y partitioning and O_3 production.

3.2 Simulation of N_2O_5 and $ClNO_2$ with N_2O_5 uptake and Cl activation

3.2.1 Comparison of simulated N_2O_5 and $ClNO_2$ with observation

The average observed and simulated (HET+Cl case) concentrations of N_2O_5 and $ClNO_2$ were calculated for each night, as shown in Fig. 2. The mean observed N_2O_5 concentrations for each night varied from 0.02 to 0.74 ppb during the study period, while the average simulated N_2O_5 values from the HET+Cl case were between 0.02 and 0.35 ppb. The HET+Cl case

Atmos. Chem. Phys. Discuss., doi:10.5194/acp-2016-412, 2016
Manuscript under review for journal Atmos. Chem. Phys.
Published: 1 June 2016

reproduced the order of N_2O_5 concentrations but underestimated them within a factor of three. For $ClNO_2$, the average observed concentrations varied from 0.01 to 0.39 ppb, whilst the mean simulated values for each night varied between 0.05 and 0.42 ppb. The HET+Cl case reproduced the order of $ClNO_2$ concentrations with an overestimate mostly within a factor of four. The simulated and observed hourly concentrations of N_2O_5 and $ClNO_2$ are shown in Fig. S2, indicating that the HET+Cl case well captured the temporal variations of these two compounds.

The under-simulated N_2O_5 and over-simulated $ClNO_2$ values in the HET+Cl case point to the underestimation of the sources and/or the overestimation of the sink of N_2O_5 and the overestimation of the production of $ClNO_2$. As shown in section 3.1, the simulated NO_2 and O_3 levels in the HK-PRD region are lower than the observations, which results in lower production of N_2O_5; the simulated $PM_{2.5}$ concentrations are higher than the observed values which would lead to an overestimate of N_2O_5 heterogeneous loss. The observation-derived N_2O_5 uptake coefficients at the TMS site (Brown et al., 2016) varied from 0.004 to 0.029 with an average value of 0.014, whilst the simulated uptake coefficients ranged from 0.008 to 0.031 with an average of 0.019, which suggests that the HET+Cl simulation generally overestimates N_2O_5 uptake coefficients, which causes further overestimation of the loss of N_2O_5. The overestimated loss of N_2O_5 on aerosol inherently overestimated the production of $ClNO_2$. The parameterisations used in this study are likely to overestimate the $ClNO_2$ yield (Kim et al., 2014; Ryder et al., 2015), which would further overestimate the production of $ClNO_2$.

Discrepancies between the measured and simulated N_2O_5 and $ClNO_2$ levels have also been reported in previous model studies. Lowe et al. (2015) used the same parameterisations for N_2O_5 uptake that we applied in our study and showed slightly higher average simulated N_2O_5 values along two flight tracks but a factor of 1-2 lower simulated N_2O_5 in another flight. They noted that the underestimated N_2O_5 could be attributed to inaccuracies in the meteorological simulation. Sarwar et al. (2012) used the parameterisation for N_2O_5 uptake proposed by Davis et al. (2008) and by Bertram and Thornton et al. (2009) and yielded a slightly higher simulated peak value of $ClNO_2$ than the observed value in field studies conducted at different times from the model simulations. The authors attributed the overestimate of $ClNO_2$ to the overestimated N_2O_5 uptake in the parameterisations. Sarwar et al. (2014) predicted lower peak values of $ClNO_2$ than the observations and suggested that the underestimated $ClNO_2$ could be attributed to a relatively low model resolution (108 km).

3.2.2 Spatial distribution of average simulated N_2O_5 and $ClNO_2$

Figure 3a and 3c show the average mixing ratios of N_2O_5 and $ClNO_2$ during the entire simulation period within the lowest 1000 m (the approximate height of the PBL at noon) in southern China in the HET+Cl case. Elevated levels of N_2O_5 (>0.10 ppb) and $ClNO_2$ (>0.25 ppb) were predicted in the areas downwind of the PRD, as a result of the transport of pollutant enriched air masses towards the south-west of the PRD by the prevailing north-easterly winds. The areas with the highest simulated N_2O_5 and $ClNO_2$ values did not cover the TMS site at which the highest ever reported N_2O_5 and $ClNO_2$ values were observed

Atmos. Chem. Phys. Discuss., doi:10.5194/acp-2016-412, 2016
Manuscript under review for journal Atmos. Chem. Phys.
Published: 1 June 2016

Atmospheric Chemistry and Physics Discussions

(Brown et al., 2016; Wang et al., 2016), which supports our speculation that the locations downwind of the PRD under the dominant north-easterly winds may frequently have higher levels of $ClNO_2$.

The vertical distributions of N_2O_5 and $ClNO_2$ in the vertical domain (as described in section 2.3.1) are shown in Fig. 3b and 3d. Elevated levels of N_2O_5 (> 0.10 ppb) were predicted up to around 1000 m a.g.l., with the highest N_2O_5 level (>0.25 ppb) mostly between 400-800m a.g.l., probably due to suppression of NO_3 (and N_2O_5) by NO in the lowest several hundred meters over the urban area, as shown in Fig. S3. Elevated levels of $ClNO_2$ (>0.25 ppb) were simulated up to 1000 m a.g.l., with the highest $ClNO_2$ values (>1.00 ppb) mostly concentrated within the near-surface layer of 0-200 m a.g.l. The vertical distribution of $ClNO_2$ was consistent with the vertical profile of chloride, as shown in Fig. S4. The simulated vertical distribution of N_2O_5 and $ClNO_2$ are similar to those of Sarwar et al. (2012), which showed that simulated N_2O_5 peaked at 200-400 m a.g.l., and simulated $ClNO_2$ peaked at the surface and stretched up to 400 m a.g.l. in several U.S. cities at dawn.

3.2.3 Dynamic evolutions in cases with typical and extreme meteorological conditions

We examine the time evolution of the spatial distribution of $ClNO_2$ in two cases. In the typical case (the night of December 1/2), southern China was dominated by consistent north-easterly winds which represented the average dynamic conditions during the study period, while in the extreme case (the night of December 3/4), the air-flow over the region abruptly changed. Note that in this extreme case, the highest ever-reported $ClNO_2$ levels were observed at the TMS site, and the back trajectories and observations of chemical species pointed to the transport to the site of well-processed plumes from the PRD with enriched anthropogenic chloride and other pollutants (Wang et al., 2016).

In the typical case, consistent north-easterly winds controlled southern China throughout the night (Fig. 4). At the beginning of the night (18:00, local time (LT)), $ClNO_2$ began to build up near the urban area (Fig. 4a) and near the surface (Fig. 4b); at midnight (00:00, LT), the air with an elevated level of $ClNO_2$ moved to coastal areas (Fig. 4c) and accumulated near the surface (Fig. 4d); at dawn (06:00, LT), the peak $ClNO_2$ level was predicted over the open sea (Fig. 4e), and pumped up to higher altitudes with the peak value near the surface (Fig. 4f), due to the higher boundary layer height over the ocean, as shown in Fig. S5.

In the extreme case, at the beginning of the evening (18:00, LT), southern China had unfavourable dispersion conditions over the land, including inconsistent wind directions and low wind speeds. The air pollutants emitted from the PRD slowly swirled over it, as shown in Fig. 5a, resulting in a longer 'cooking' time for $ClNO_2$ production. The vertical distribution (Fig. 5b) shows that $ClNO_2$-enriched air stretched from the ground up to 800m a.g.l. The enhanced production of $ClNO_2$ is believed to be partially responsible for the highest $ClNO_2$ mixing ratios measured at the TMS site at this night. At midnight (00:00, LT), inconsistent wind directions presented between land and sea areas: northerly winds dominated over the land area, while north-easterly winds dominated over the sea, leading to relatively slow motion of the $ClNO_2$-enriched plume from the land towards the ocean (Fig. 5c). The vertical distribution (Fig. 5d) suggests that $ClNO_2$ built up within the residue layer. At dawn (06:00,

Atmos. Chem. Phys. Discuss., doi:10.5194/acp-2016-412, 2016
Manuscript under review for journal Atmos. Chem. Phys.
Published: 1 June 2016

Atmospheric Chemistry and Physics Discussions

LT), the north-easterly wind regained control over the land areas, and the air with the elevated level of $ClNO_2$ (>2.00 ppb) was driven towards the ocean, as shown in Fig. 5e. The vertical distribution (Fig. 5f) shows that the peak $ClNO_2$ concentration was predicted to be in the residue layer at ~300m a.g.l. The changes of wind flow over the region during this night resulted in abnormal changes in the history of the air masses that reached the TMS site and led to the abrupt changes in the air pollutants concentrations observed there (see Wang et al., 2016 for details).

From these results, it can be seen that the vertical distributions of $ClNO_2$ demonstrated distinct features in the two cases. To understand the underlying cause, it is of significance to measure the vertical profiles of $ClNO_2$ under various meteorological conditions. In addition, during the extreme event, the location with the highest predicted $ClNO_2$ (>2.00 ppb) was not at the TMS site (>1.00 ppb), but was located in the western parts of the PRD (i.e., the cites of Jiangmen and Zhaoqing), which supports the contention that the $ClNO_2$ concentrations at other locations could be even higher than those observed at the TMS site (Wang et al., 2016). It would be of great interest to conduct measurements at the areas where the highest $ClNO_2$ concentrations are predicted.

3.3 Impacts of N_2O_5 heterogeneous uptake and Cl activation on NO_x, total nitrate and O_3

3.3.1 Impacts in the horizontal and vertical domains

Figure 6 shows the simulation results for the average NO, NO_2, total nitrate and O_3 concentrations within the PBL (<1000m) in the Base case, and the difference of the results between the HET+Cl and Base cases in the horizontal domain. Elevated levels of NO (up to 26.18 ppb; Fig. 6a), NO_2 (up to 29.18 ppb; Fig. 6c), total nitrate (up to 23.43 μg m^{-3}; Fig. 6e), and O_3 (up to 44.50 ppb; Fig. 6g) were predicted in southern China in the Base case. With the prevailing north-easterly wind, the pollutants emitted from the PRD were transported towards the south-west, resulting in the most polluted regions being the PRD and its south-westerly downwind areas. After addition of the N_2O_5 uptake and Cl activation processes, the NO (Fig. 6b) and NO_2 (Fig. 6d) levels were significantly decreased in the entire domain by up to 1.93 ppb (~ 7.4%) and 4.73 ppb (~ 16.2%), respectively. The regions with greater impacts on the NO and NO_2 due to the added processes were mostly urban and suburban areas with large emissions of NO_x. A significant portion of NO_x was transformed into total nitrate, which increased by as much as 13.45 μg m^{-3} (~ 57.4%) through the heterogeneous uptake of N_2O_5 (see Fig. 6f). As can be seen in Fig. 6h, the N_2O_5 uptake and Cl activation noticeably increased O_3 levels across southern China, with a maximum increase up to 7.23 ppb (~16.3%). It is worth noting that in addition to the urban and suburban areas, the O_3 levels over the rural and coastal areas was also significantly affected by the added processes.

Figure 7 shows the average simulated NO, NO_2, total nitrate and O_3 values in the Base case, and the difference in the results between the Base and HET+Cl cases in the vertical domain. NO and NO_2 were concentrated within 800 m a.g.l. over the PRD and in downwind areas (see Fig. 7a and 7c). Total nitrate accumulated near the ground and stretched up to 800 m a.g.l. (Fig. 7e). Due to the titration effect of NO, relatively low average values of O_3 were simulated over urban areas (Fig. 7g). As shown

Atmos. Chem. Phys. Discuss., doi:10.5194/acp-2016-412, 2016
Manuscript under review for journal Atmos. Chem. Phys.
Published: 1 June 2016

Atmospheric Chemistry and Physics Discussions

in Fig. 7b and 7d, the N_2O_5 uptake and Cl activation decreased the NO and NO_2 levels across the vertical domain, with the largest impacts seen in the near-surface layer (0-400 m a.g.l.) over the PRD. The lost NO and NO_2 were mostly transformed into total nitrate, which increased remarkably in the near-surface layer (Fig. 7f). The impacts of N_2O_5 uptake and Cl activation on the O_3 level varied with altitude: the O_3 increased throughout the lowest 800 m with the largest enhancement near the ground, whereas it decreased above 1000 m a.g.l. (Fig. 7h). The changes in the O_3 were attributed to the combined effects of NO_x loss due to N_2O_5 uptake and Cl atom production due to Cl activation, both of which have nonlinear impacts on O_3 production. The relative contribution of N_2O_5 uptake versus Cl activation on the NO, NO_2, total nitrate and O_3 concentrations will be discussed in the following section.

3.3.2 Relative contribution of N_2O_5 heterogeneous uptake versus Cl activation

To understand the relative contribution of N_2O_5 uptake and Cl activation, we conducted a sensitivity case (HET case as listed in Table 2) in which only nitrate was produced via N_2O_5 uptake. The differences in the simulations between the Base and HET cases represent the effects of N_2O_5 uptake, while those between the HET and HET+Cl cases represent the effects of Cl activation.

As shown in Fig. 8a and 8c, the mere consideration of nitrate production from N_2O_5 uptake led to decreases in NO and NO_2 by up to 1.11 ppb and 4.28 ppb, respectively. In addition, most of the lost NO_x was transformed into total nitrate which increased by as much as 14.92 μg m^{-3} (Fig. 8e). These results are similar to those of Lowe et al. (2015), who suggested that the nitrate in PM_{10} was enhanced by up to 31.4% (increasing from 3.5 μg Kg^{-1} to 4.6 μg kg^{-1} at night) after considering the heterogeneous uptake processes of N_2O_5. The N_2O_5 uptake increased the O_3 levels by as much as 3.10 ppb in urban and suburban areas and decreased the O_3 by up to 1.47 ppb in rural and coastal areas (Fig. 8g), due to the nonlinearity of O_3 production, which are similar to the findings of Riemer et al. (2003) indicating that the N_2O_5 uptake resulted in an increase in the O_3 level in high-NO_x areas and a decrease in low-NO_x areas.

The further addition of Cl activation led to decreases in the NO level by as much as 0.96 ppb, as shown in Fig. 8b, and increases in NO_2 by up to 0.72 ppb, as shown in Fig. 8d. The Cl activation slightly decreased the total nitrate by up to 2.35 μg m^{-3} (Fig. 8f), because a fraction of N_2O_5 was consumed to produce $ClNO_2$ in competition with nitrate production. The simulated O_3 was significantly increased throughout the domain by as much as 4.54 ppb (Fig. 8h), which could be attributed to the effects of the activation of Cl radicals that initiated VOCs degradation and O_3 formation. The increase in the O_3 further enhanced the oxidation of NO into NO_2, and the recycling of NO_2 via $ClNO_2$ photolysis also contributed to the increase in NO_2.

3.4 Impacts of N_2O_5 uptake and Cl activation on NO_y partitioning

The composition and partitioning of NO_y affect the spatial range that nitrogenous species can reach after emission, and are therefore of great importance in atmospheric chemistry (Bertram et al., 2013). The average concentration of NO_y altered

Atmos. Chem. Phys. Discuss., doi:10.5194/acp-2016-412, 2016
Manuscript under review for journal Atmos. Chem. Phys.
Published: 1 June 2016

modestly within the PBL over domain 2 with the addition of N_2O_5 uptake and Cl activation (12.24 ppb and 11.42 ppb in the Base and HET+Cl cases, respectively). The fractions of each species in NO_y, however, were substantially affected. The NO_y partition was calculated over domain 2 for the Base and HET+Cl cases (see Fig 9). The percentage of N_2O_5 in NO_y decreased from 7.80% in the Base case to 1.01% in the HET+Cl case, and that for NO_3 decreased from 0.38% to 0.09%. The N_2O_5 uptake and Cl activation reduced the fraction of NO from 9.59% to 6.84% and that of NO_2 from 51.07% to 35.17%. The percentage of total nitrate (nitrate + HNO_3) in NO_y was significantly increased from 27.5% (=9.6%+17.9%) to 48.6% (=16.0%+32.6%). The added processes also introduced a new NO_y species, $ClNO_2$, which accounted for 3.47% in the HET+Cl case. The decrease in the NO_3 level caused by N_2O_5 heterogeneous uptake would suppress the night-time chemistry of NO_3 and VOCs. The N_2O_5 uptake transferred a significant portion of NO_x to total nitrate, reducing the lifetime and reaching range of NO_x-enriched plumes and thus affecting the NO_x-VOCs-O_3 photochemistry. The new species in the HET+Cl case, $ClNO_2$, contributed a non-negligible part of NO_y, and extended the lifetime and reaching range of reactive nitrogen.

3.5 Sensitivity of $ClNO_2$ concentration to chlorine emission

The production of $ClNO_2$ depends on the chloride concentration in aerosol according to the parameterisation used in this study (Bertram and Thornton, 2009). The only available chlorine EI for China is taken from a global dataset with a relatively low resolution (1°x1°) and for the year of 1990 (Keene et al., 1999). To test the sensitivity of the $ClNO_2$ production to Cl emissions, we conducted two simulations in which the RCEI emission were reduced by half (HET+Cl+0.5RCEI) and doubled (HET+Cl+2.0RCEI). The simulations show that the ambient chloride concentrations responded almost linearly to the applied chlorine emissions (data not shown). The simulated $ClNO_2$ has a similar temporal pattern in different Cl emissions (Fig. S6). The $ClNO_2$ concentrations have positive but not linear correlation to Cl emission changes. As shown in Fig. 10, halving the Cl emissions leads to a 31% reduction in the simulated $ClNO_2$ level, whereas doubling the Cl emissions results in an average 31% increase of $ClNO_2$. The results indicate that simulation of $ClNO_2$ production is sensitive to chlorine emission. Therefore, future studies are needed to develop an up-to-date anthropogenic chlorine EI in China to better model $ClNO_2$ production, and to quantify its impact on atmospheric chemistry and air quality.

4 Summary and conclusions

In this study, a state-of-the-art chemical transport model (WRF-Chem) was further developed by incorporation of a widely-used aerosol thermodynamics model (ISORROPIA II), parameterisation of heterogeneous uptake of N_2O_5 and $ClNO_2$ production, and gas-phase chlorine chemistry. The revised model was used to simulate the spatial distributions of N_2O_5 and $ClNO_2$ and the impacts on O_3 and NO_y partitioning over the HK-PRD region where high levels of N_2O_5 and $ClNO_2$ had been observed. The revised model was able to capture the temporal patterns and the magnitudes of the observed N_2O_5 and $ClNO_2$ at a mountain-top site in Hong Kong, but tended to under-simulate N_2O_5 and over-simulate $ClNO_2$ because of the

underestimates of N_2O_5 sources and overestimates of N_2O_5 sink and $ClNO_2$ production. Model simulations show that under average meteorological conditions, high values of N_2O_5 and $ClNO_2$ are concentrated in the south-west region to the urban areas of the PRD and vertically peak within the layer of 400-800 m a.g.l. and 0-200 m a.g.l, respectively. At the night of December 3/4 when the highest ever-reported $ClNO_2$ (4.7 ppb) was observed, the model suggested that the high levels of $ClNO_2$ were concentrated in the residue layer (~300m a.g.l.) above the study region. The model simulations suggested that the region downwind of the urban PRD may experience higher levels of $ClNO_2$ than that observed at the TMS site. N_2O_5 uptake and Cl activation significantly decreased the levels of NO and NO_2 by up to 1.93 ppb (~7.4%) and 4.73 ppb (~16.2%), respectively, but increased the total nitrate level by as much as 13.45 μg m^{-3} (~ 57.4%) and the O_3 by up to 7.23 ppb (~16.3%) within the PBL. Our results demonstrate the significant impacts of N_2O_5 uptake and $ClNO_2$ production on NO_x lifetime, secondary nitrate production, and O_3 formation and underscore the necessity of considering these processes in air quality models. Our simulations of $ClNO_2$ levels over southern China are sensitive to chlorine emissions, which suggests the need to develop a more reliable emission inventory of chlorine for better quantification of the N_2O_5/$ClNO_2$ chemistry and their impacts over China.

Acknowledgements:

The authors would like to thank China National Meteorological Center and Hong Kong Observatory for providing the meteorological data and Hong Kong Environmental Protection Department for providing the routine air pollutants measurement data and the emission inventory in Hong Kong. This study is supported by a Hong Kong Polytechnic University PhD studentship, General Research Fund of Hong Kong Research Grants Council (PolyU 153026/14P), and Collaborative Research Fund of the Hong Kong Research Grants Council (C5022-14G). Both the data and source code of the revised model used in this study are available from the corresponding author (cetwang@polyu.edu.hk) upon request.

Reference:

Ahmadov, R., McKeen, S.A., Robinson, A.L., Bahreini, R., Middlebrook, A.M., Gouw, J.D., Meagher, J., Hsie, E.Y., Edgerton, E., Shaw, S. and Trainer, M.: A volatility basis set model for summertime secondary organic aerosols over the eastern United States in 2006, J. Geophys. Res. Atmos., 117, doi: 10.1029/2011JD016831, 2012.

Anttila, T., Kiendler-Scharr, A., Tillmann, R. and Mentel, T.F.: On the reactive uptake of gaseous compounds by organic-coated aqueous aerosols: Theoretical analysis and application to the heterogeneous hydrolysis of N_2O_5, The J. Phys. Chem A, 110, 10435-10443, 2006.

Archer-Nicholls, S., Lowe, D., Utembe, S., Allan, J., Zaveri, R.A., Fast, J.D., Hodnebrog, Ø., Denier van der Gon, H. and McFiggans, G.: Gaseous chemistry and aerosol mechanism developments for version 3.5.1 of the online regional model, WRF-Chem, Geosci. Model Dev., 7, 2557-2579, 2014.

Atkinson, R.: Atmospheric chemistry of VOCs and NO_x, Atmos. Environ., 34, 2063-2101, 2000.

Atkinson, R., Baulch, D.L., Cox, R.A., Crowley, J.N., Hampson, R.F., Hynes, R.G., Jenkin, M.E., Rossi, M.J. and Troe, J.: Evaluated kinetic and photochemical data for atmospheric chemistry: Volume III–gas phase reactions of inorganic halogens, Atmos. Chem. Phys., 7, 981-1191, 2007.

Atkinson, R., Baulch, D.L., Cox, R.A., Crowley, J.N., Hampson, R.F., Hynes, R.G., Jenkin, M.E., Rossi, M.J., Troe, J. and Wallington, T.J.: Evaluated kinetic and photochemical data for atmospheric chemistry: Volume IV–gas phase reactions of organic halogen species, Atmos. Chem. Phys., 8, 4141-4496, 2008.

Bertram, T.H. and Thornton, J.A.: Toward a general parameterization of N_2O_5 reactivity on aqueous particles: the competing effects of particle liquid water, nitrate and chloride, Atmos. Chem. Phys., 9, 8351-8363, 2009.

Bertram, T.H., Perring, A.E., Wooldridge, P.J., Dibb, J., Avery, M.A. and Cohen, R.C.: On the export of reactive nitrogen from Asia: NO_x partitioning and effects on ozone, Atmos. Chem. Phys., 13, 4617-4630, 2013.

Brown, S.S. and Stutz, J.: Nighttime radical observations and chemistry, Chem. Soc. Rev., 41, 6405-6447, 2012.

Brown, S.S., Dubé, W.P., Tham, Y.J., Zha, Q., Xue, L., Poon, S., Wang, Z., Blake, D.R., Tsui, W., Parrish, D.D. and Wang, T.: Nighttime chemistry at a high altitude site above Hong Kong, J. Geophys. Res. Atmos., 121, doi: 10.1002/2015JD024566, 2016.

Chang, W.L., Bhave, P.V., Brown, S.S., Riemer, N., Stutz, J. and Dabdub, D.: Heterogeneous atmospheric chemistry, ambient measurements, and model calculations of N_2O_5: A review, Aerosol Sci. Tech., 45, 665-695, 2011.

Chen, F. and Dudhia, J.: Coupling an advanced land surface-hydrology model with the Penn State-NCAR MM5 modeling system. Part I: Model implementation and sensitivity, Mon. Weather Rev., 129, 569-585, 2001.

Davis, J.M., Bhave, P.V. and Foley, K.M.: Parameterization of N_2O_5 reaction probabilities on the surface of particles containing ammonium, sulfate, and nitrate, Atmos. Chem. Phys., 8, 5295-5311, 2008.

Dentener, F.J. and Crutzen, P.J.: Reaction of N_2O_5 on tropospheric aerosols: Impact on the global distributions of NO_x, O_3, and OH, J. Geophys. Res. Atmos., 98, 7149-7163, 1993.

Evans, M.J. and Jacob, D.J.: Impact of new laboratory studies of N_2O_5 hydrolysis on global model budgets of tropospheric nitrogen oxides, ozone, and OH, Geophys. Res. Lett., 32, doi: 10.1029/2005GL022469, 2005.

Finlayson-Pitts, B.J., Ezell, M.J. and Pitts, J.N.: Formation of chemically active chlorine compounds by reactions of atmospheric NaCl particles with gaseous N_2O_5 and $ClONO_2$, Nature, 337, 241-244, 1989.

Fountoukis, C. and Nenes, A.: ISORROPIA II: a computationally efficient thermodynamic equilibrium model for K^+–Ca^{2+}–Mg^{2+}–NH^{4+}–Na^+–SO_4^{2-}–NO_3^-–Cl^-–H_2O aerosols, Atmos. Chem. Phys., 7, 4639-4659, 2007.

Gong, S.L., Barrie, L.A. and Lazare, M.: Canadian Aerosol Module (CAM): A size-segregated simulation of atmospheric aerosol processes for climate and air quality models: 2. Global sea-salt aerosol and its budgets, J. Geophys. Res. Atmos., 107, doi: 10.1029/2001JD002004, 2002.

Grell, G.A. and Dévényi, D.: A generalized approach to parameterizing convection combining ensemble and data assimilation techniques, Geophys. Res. Lett., 29, doi: 10.1029/2002GL015311, 2002.

Grell, G.A., Peckham, S.E., Schmitz, R., McKeen, S.A., Frost, G., Skamarock, W.C. and Eder, B.: Fully coupled "online" chemistry within the WRF model, Atmos. Environ., 39, 6957-6975, 2005.

Guenther, A., Zimmerman, P. and Wildermuth, M.: Natural volatile organic compound emission rate estimates for US woodland landscapes, Atmos. Environ., 28, 1197-1210, 1994.

Hong, S.Y., Noh, Y. and Dudhia, J.: A new vertical diffusion package with an explicit treatment of entrainment processes, Mon. Weather Rev., 134, 2318-2341, 2006.

Iacono, M.J., Delamere, J.S., Mlawer, E.J., Shephard, M.W., Clough, S.A. and Collins, W.D.: Radiative forcing by long-lived greenhouse gases: Calculations with the AER radiative transfer models, J. Geophys. Res. Atmos., 113, doi: 10.1029/2008JD009944, 2008.

Keene, W., Khalil, M.A.K., Erickson, D., McCulloch, A., Graedel, T.E., Lobert, J.M., Aucott, M.L., Gong, S.L., Harper, D.B., Kleiman, G., Midgley, P., Moore, R.M., Seuzaret, C., Sturges, W.T., Benkovitz, C.M., Koropalov, V., Barrie, L.A. and Li, Y.F.: Composite global emissions of reactive chlorine from anthropogenic and natural sources: Reactive Chlorine Emissions Inventory, J. Geophys. Res. Atmos., 104, 8429-8440, 1999.

Kim, M.J., Farmer, D.K. and Bertram, T.H.: A controlling role for the air− sea interface in the chemical processing of reactive nitrogen in the coastal marine boundary layer, P. Natl. Acad. Sci. USA, 111, 3943-3948, 2014.

Li, Y., An, J., Min, M., Zhang, W., Wang, F. and Xie, P.: Impacts of HONO sources on the air quality in Beijing, Tianjin and Hebei Province of China, Atmos. Environ., 45, 4735-4744, 2011.

Lin, Y.L., Farley, R.D. and Orville, H.D.: Bulk parameterization of the snow field in a cloud model, J. Clim. Appl. Meteorol., 22, 1065-1092, 1983.

Liu, F., Zhang, Q., Tong, D., Zheng, B., Li, M., Huo, H. and He, K.B.: High-resolution inventory of technologies, activities, and emissions of coal-fired power plants in China from 1990 to 2010, Atmos. Chem. Phys., 15, 13299-13317, 2015.

Lowe, D., Archer-Nicholls, S., Morgan, W., Allan, J., Utembe, S., Ouyang, B., Aruffo, E., Le Breton, M., Zaveri, R.A., Di Carlo, P., Percival, C., Coe, H., Jones, R. and McFiggans, G.: WRF-Chem model predictions of the regional impacts of N_2O_5 heterogeneous processes on night-time chemistry over north-western Europe, Atmos. Chem. Phys., 15, 1385-1409, 2015.

Madronich, S.: Photodissociation in the atmosphere: 1. Actinic flux and the effects of ground reflections and clouds, J. Geophys. Res. Atmos., 92, 9740-9752, 1987.

Millero, F.J. Chemical oceanography. CRC press, Boca Raton, FL, USA, 1996.

Nenes, A., Pandis, S.N. and Pilinis, C.: ISORROPIA: A new thermodynamic equilibrium model for multiphase multicomponent inorganic aerosols, Aquat. Geochem., 4, 123-152, 1998.

Osthoff, H.D., Roberts, J.M., Ravishankara, A.R., Williams, E.J., Lerner, B.M., Sommariva, R., Bates, T.S., Coffman, D., Quinn, P.K., Dibb, J.E., Stark, H., Burkholder, J.B., Talukdar, R.K., Meagher, J., Fehsenfeld, F.C. and Brown. S.S.: High levels of nitryl chloride in the polluted subtropical marine boundary layer, Nat. Geosci., 1, 324-328, 2008.

Riedel, T.P., Wolfe, G.M., Danas, K.T., Gilman, J.B., Kuster, W.C., Bon, D.M., Vlasenko, A., Li, S.M., Williams, E.J., Lerner, B.M., Veres, P.R., Roberts, J.M., Holloway, J.S., Lefer, B., Brown, S.S. and Thornton, J.A.: An MCM modeling study of nitryl chloride ($ClNO_2$) impacts on oxidation, ozone production and nitrogen oxide partitioning in polluted continental outflow, Atmos. Chem. Phys., 14, 3789-3800, 2014.

Riemer, N., Vogel, H., Vogel, B., Schell, B., Ackermann, I., Kessler, C. and Hass, H.: Impact of the heterogeneous hydrolysis of N_2O_5 on chemistry and nitrate aerosol formation in the lower troposphere under photosmog conditions, J. Geophys. Res. Atmos., 108, doi: 10.1029/2002JD002436, 2003.

Riemer, N., Vogel, H., Vogel, B., Anttila, T., Kiendler-Scharr, A. and Mentel, T.F.: Relative importance of organic coatings for the heterogeneous hydrolysis of N_2O_5 during summer in Europe. J. Geophys. Res. Atmos., 114, doi: 10.1029/2008JD011369, 2009.

Roberts, J.M., Osthoff, H.D., Brown, S.S., Ravishankara, A.R., Coffman, D., Quinn, P. and Bates, T.: Laboratory studies of products of N_2O_5 uptake on Cl^- containing substrates, Geophys. Res. Lett., 36, doi: 10.1029/2009GL040448, 2009.

Ryder, O.S., Campbell, N.R., Shaloski, M., Al-Mashat, H., Nathanson, G.M. and Bertram, T.H.: Role of Organics in Regulating $ClNO_2$ Production at the Air–Sea Interface, J. Phys. Chem. A, 119, 8519-8526, 2015.

Sarwar, G., Simon, H., Bhave, P. and Yarwood, G.: Examining the impact of heterogeneous nitryl chloride production on air quality across the United States, Atmos. Chem. Phys., 12, 6455-6473, 2012.

Sarwar, G., Simon, H., Xing, J. and Mathur, R.: Importance of tropospheric $ClNO_2$ chemistry across the Northern Hemisphere, Geophys. Res. Lett., 41, 4050-4058, 2014.

Shaw, W.J., Allwine, K.J., Fritz, B.G., Rutz, F.C., Rishel, J.P. and Chapman, E.G.: An evaluation of the wind erosion module in DUSTRAN, Atmos. Environ., 42, 1907-1921, 2008.

Simon, H., Kimura, Y., McGaughey, G., Allen, D.T., Brown, S.S., Coffman, D., Dibb, J., Osthoff, H.D., Quinn, P., Roberts, J.M., Yarwood, G., Kemball-Cook. S., Byun, D. and Lee, D.: Modeling heterogeneous $ClNO_2$ formation, chloride availability, and chlorine cycling in Southeast Texas, Atmos. Environ., 44, 5476-5488, 2010.

Stockwell, W.R., Kirchner, F., Kuhn, M. and Seefeld, S.: A new mechanism for regional atmospheric chemistry modeling, J. Geophys. Res. Atmos., 102, 25847-25879, 1997.

Tan, J., Duan, J., He, K., Ma, Y., Duan, F., Chen, Y., and Fu, J.: Chemical characteristics of $PM_{2.5}$ during a typical haze episode in Guangzhou, J. Environ. Sci., 21, 774-781, 2009.

Tao, J., Zhang, L., Ho, K., Zhang, R., Lin, Z., Zhang, Z., Lin, M., Cao, J., Liu, S. and Wang, G.: Impact of $PM_{2.5}$ chemical compositions on aerosol light scattering in Guangzhou—the largest megacity in South China, Atmos. Res., 135, 48-58, 2014.

Tham, Y.J., Yan, C., Xue, L., Zha, Q., Wang, X. and Wang, T.: Presence of high nitryl chloride in Asian coastal environment and its impact on atmospheric photochemistry, Chin. Sci. Bull., 59, 356-359, 2014.

Thornton, J.A., Kercher, J.P., Riedel, T.P., Wagner, N.L., Cozic, J., Holloway, J.S., Dubé, W.P., Wolfe, G.M., Quinn, P.K., Middlebrook, A.M., Alexander, B. and Brown, S.S.: A large atomic chlorine source inferred from mid-continental reactive nitrogen chemistry, Nature, 464, 271-274, 2010.

Wang, T., Wei, X.L., Ding, A.J., Poon, C.N., Lam, K.S., Li, Y.S., Chan, L.Y. and Anson, M.: Increasing surface ozone concentrations in the background atmosphere of Southern China, 1994–2007, Atmos. Chem. Phys., 9, 6217-6227, 2009.

Wang, T., Tham, Y.J., Xue, L., Li, Q., Zha, Q., Wang, Z., Poon, S.C.N., Dubé, W.P., Blake, D.R., Louie, P.K.K., Luk, C.W.Y., Tsui, W. and Brown, S.S.: Observations of nitryl chloride and modeling its source and effect on ozone in the planetary boundary layer of southern China, J. Geophys. Res. Atmos., 121, doi: 10.1002/2015JD024556, 2016.

Wang, X., Wang, T., Yan, C., Tham, Y.J., Xue, L., Xu, Z. and Zha, Q.: Large daytime signals of N_2O_5 and NO_3 inferred at 62 amu in a TD-CIMS: chemical interference or a real atmospheric phenomenon?, Atmos. Meas. Tech., 7, 1-12, 2014.

Wedepohl, K.H.: The composition of the continental crust. Geochim. Cosmochim. Ac., 59, 1217-1232, 1995.

Xu, Z., Wang, T., Xue, L.K., Louie, P.K., Luk, C.W., Gao, J., Wang, S.L., Chai, F.H. and Wang, W.X.: Evaluating the uncertainties of thermal catalytic conversion in measuring atmospheric nitrogen dioxide at four differently polluted sites in China, Atmos. Environ., 76, 221-226, 2013.

Xue, L.K., Saunders, S.M., Wang, T., Gao, R., Wang, X.F., Zhang, Q.Z. and Wang, W.X.: Development of a chlorine chemistry module for the Master Chemical Mechanism, Geosci. Model Dev., 8, 3151-3162, 2015.

Zhang, L., Wang, T., Lv, M. and Zhang, Q.: On the severe haze in Beijing during January 2013: Unraveling the effects of meteorological anomalies with WRF-Chem, Atmos. Environ., 104, 11-21, 2015.

Zhang, L., Wang, T., Zhang, Q., Zheng, J., Xu, Z. and Lv, M.: Potential Sources of Nitrous Acid (HONO) and Their Impacts on Ozone: A WRF-Chem study in a Polluted Subtropical Region, J. Geophys. Res. Atmos., 121, doi: 10.1002/2015JD024468, 2016.

Zhang, Q., Streets, D.G., Carmichael, G.R., He, K.B., Huo, H., Kannari, A., Klimont, Z., Park, I.S., Reddy, S., Fu, J.S., Chen, D., Duan, L., Lei, Y., Wang, L.T. and Yao, Z.L.: Asian emissions in 2006 for the NASA INTEX-B mission. Atmos. Chem. Phys., 9, 5131-5153, 2009.

Atmos. Chem. Phys. Discuss., doi:10.5194/acp-2016-412, 2016
Manuscript under review for journal Atmos. Chem. Phys.
Published: 1 June 2016

Atmospheric Chemistry and Physics Discussions

Table 1. Model configuration

WRF-Chem modules	Parameterization options	Reference
Land surface	Noah Land Surface Model	Chen and Dudhia (2001)
PBL scheme	YSU	Hong et al. (2006)
Microphysics	Purdue Lin Scheme	Lin et al. (1983)
Cumulus	Grell 3-D ensemble	Grell and Devenyi (2002)
Shortwave and longwave radiation	RRTMG	Iacono et al. (2008)
Gas chemistry	RACM_ESRL	Updated version based on Stockwell et al. (1997)
Aerosol	MADE/VBS	Ahmadov et al. (2012)
Photolysis	Madronich	Madronich (1987)

Table 2. Simulation cases

Cases	Aerosol thermodynamics module	N_2O_5 and $ClNO_2$ chemistry
Base	ISORROPIA II	None
HET	ISORROPIA II	N_2O_5 heterogeneous uptake, no $ClNO_2$ production
HET+Cl	ISORROPIA II	N_2O_5 heterogeneous uptake, $ClNO_2$ production and gas-phase Cl reactions

Table 3. Comparison of chemical simulation with observation for Base case

	$PM_{2.5}$ ($\mu g\ m^{-3}$)	NO_2 (ppb)	O_3 (ppb)
Observation Average	37.43	33.67	28.29
Simulation Average	48.08	28.81	15.06
Normalized Mean Bias	28.5%	-14.4%	-46.8%
Fac2	0.69	0.71	0.46

Table 4. Comparison of measured and simulated (Base) chloride

Location	Period	Average measured concentration ($\mu g\ m^{-3}$)	Average simulated concentration ($\mu g\ m^{-3}$)
GZ	2007/12/31 to 2008/1/12 normal day	1.19 [a]	2.51
GZ	2007/12/31 to 2008/1/12 haze day	8.37 [a]	2.51
SCIES, GZ	2009-2010 winter	3.30 [b]	2.13
TC, HK	2011/10/25 to 2011/12/7	1.10 [c]	0.32
TMS, HK	2013/11/15 to 2013/12/5	0.37 [d]	0.14

a: Tan et al., 2009; b: Tao et al., 2014; c: unpublished data; d: Wang et al., 2016.

Atmos. Chem. Phys. Discuss., doi:10.5194/acp-2016-412, 2016
Manuscript under review for journal Atmos. Chem. Phys.
Published: 1 June 2016

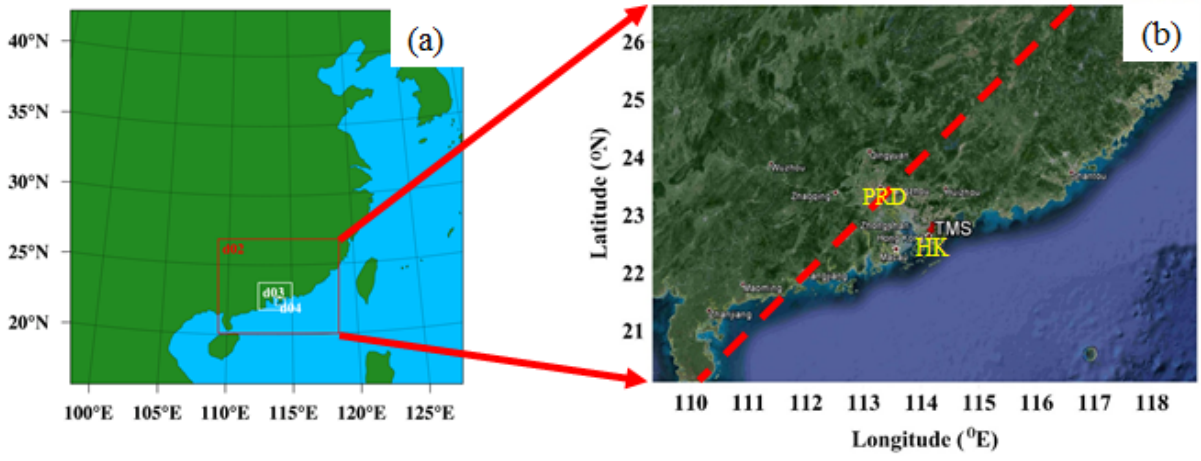

Figure 1. (a) Domain settings of WRF-chem simulations, and (b) the terrain in domain 2 (southern China). The red dotted line represents the vertical domain that intercepts the most polluted PRD region along the prevailing wind direction (north-east). TMS is the location of the site where N_2O_5 and $ClNO_2$ were measured. HK and PRD are the general locations of Hong Kong and Pearl River Delta region.

Atmos. Chem. Phys. Discuss., doi:10.5194/acp-2016-412, 2016
Manuscript under review for journal Atmos. Chem. Phys.
Published: 1 June 2016

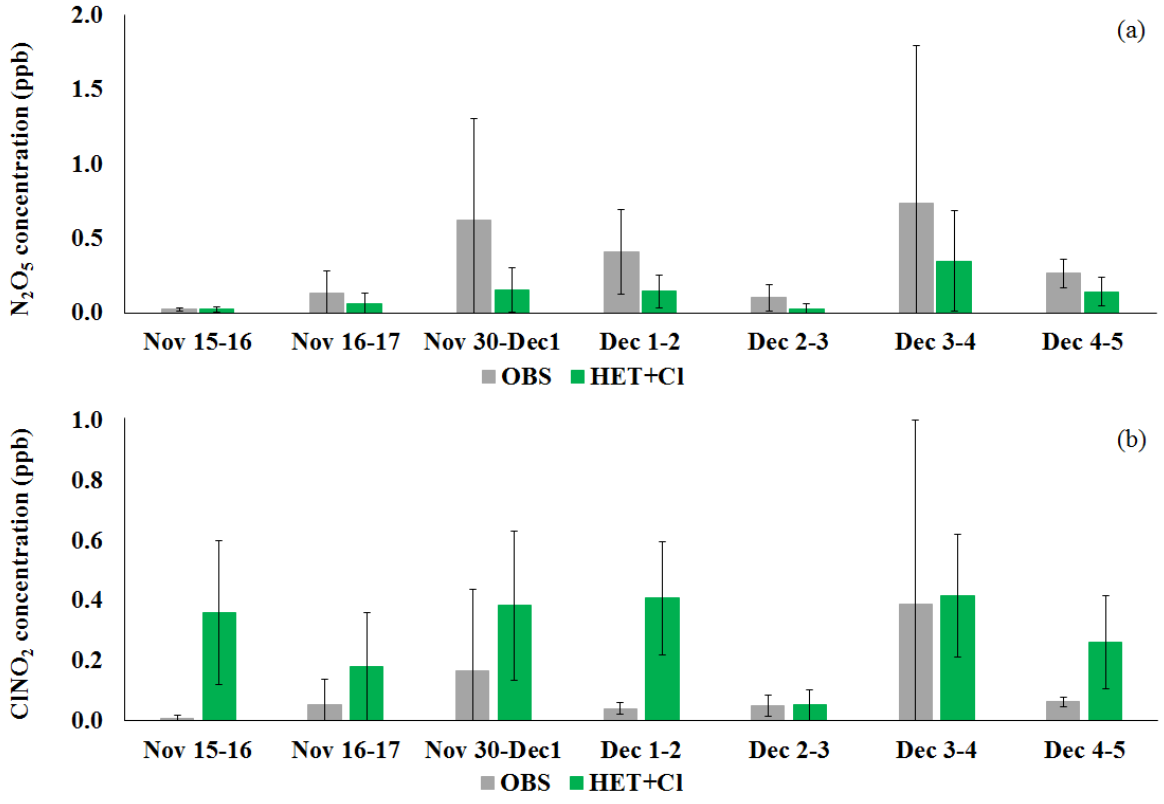

Figure 2. Comparison of simulated and observed average (a) N_2O_5 and (b) $ClNO_2$ concentrations at each night at TMS site. Error bars represent the standard deviation.

Atmos. Chem. Phys. Discuss., doi:10.5194/acp-2016-412, 2016
Manuscript under review for journal Atmos. Chem. Phys.
Published: 1 June 2016

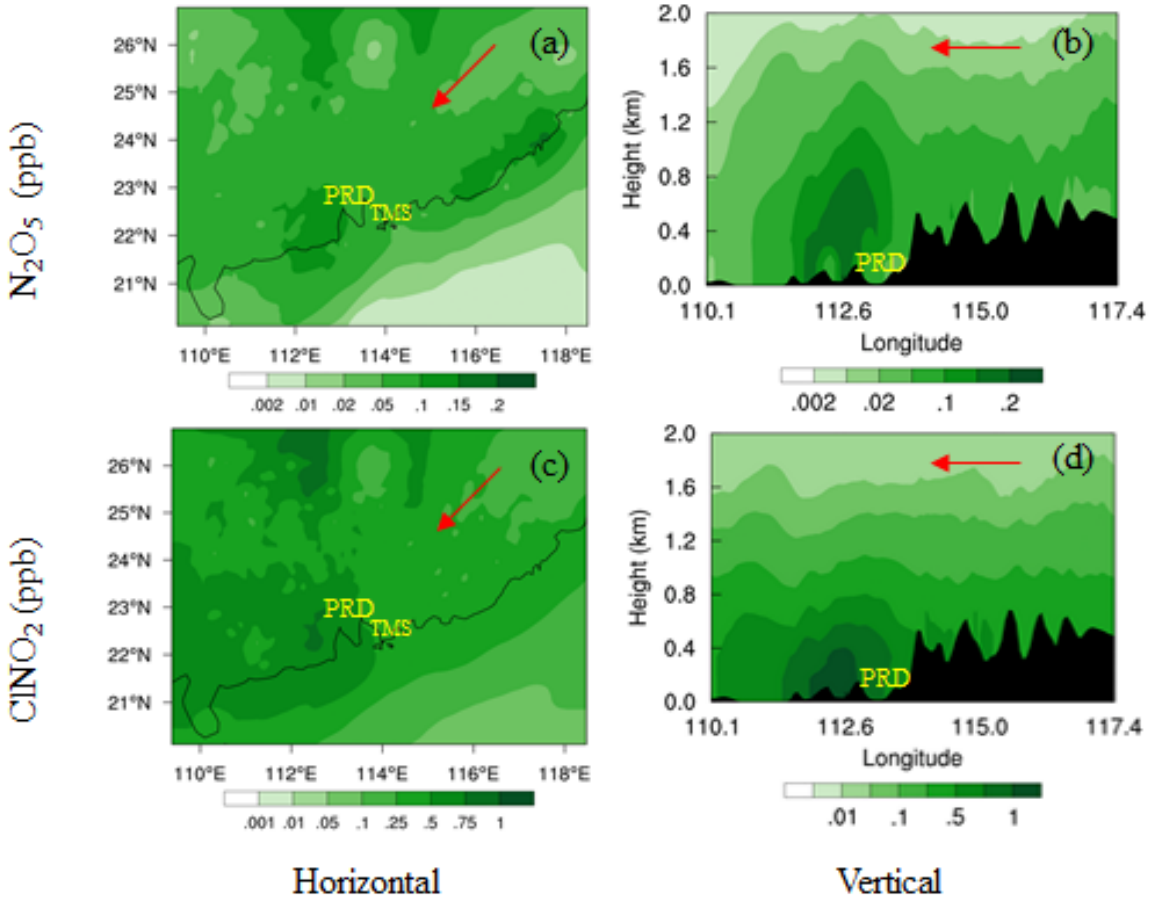

Figure 3. Horizontal distributions of (a) N_2O_5 and (c) $ClNO_2$ average mixing ratios (ppb) during the study period within the PBL from HET+Cl case; vertical distributions of (b) N_2O_5 and (d) $ClNO_2$ average mixing ratios (ppb) during the study period in the domain intercepting PRD and along the prevailing wind direction from HET+Cl case. Red arrows represent the prevailing wind direction.

Atmos. Chem. Phys. Discuss., doi:10.5194/acp-2016-412, 2016
Manuscript under review for journal Atmos. Chem. Phys.
Published: 1 June 2016

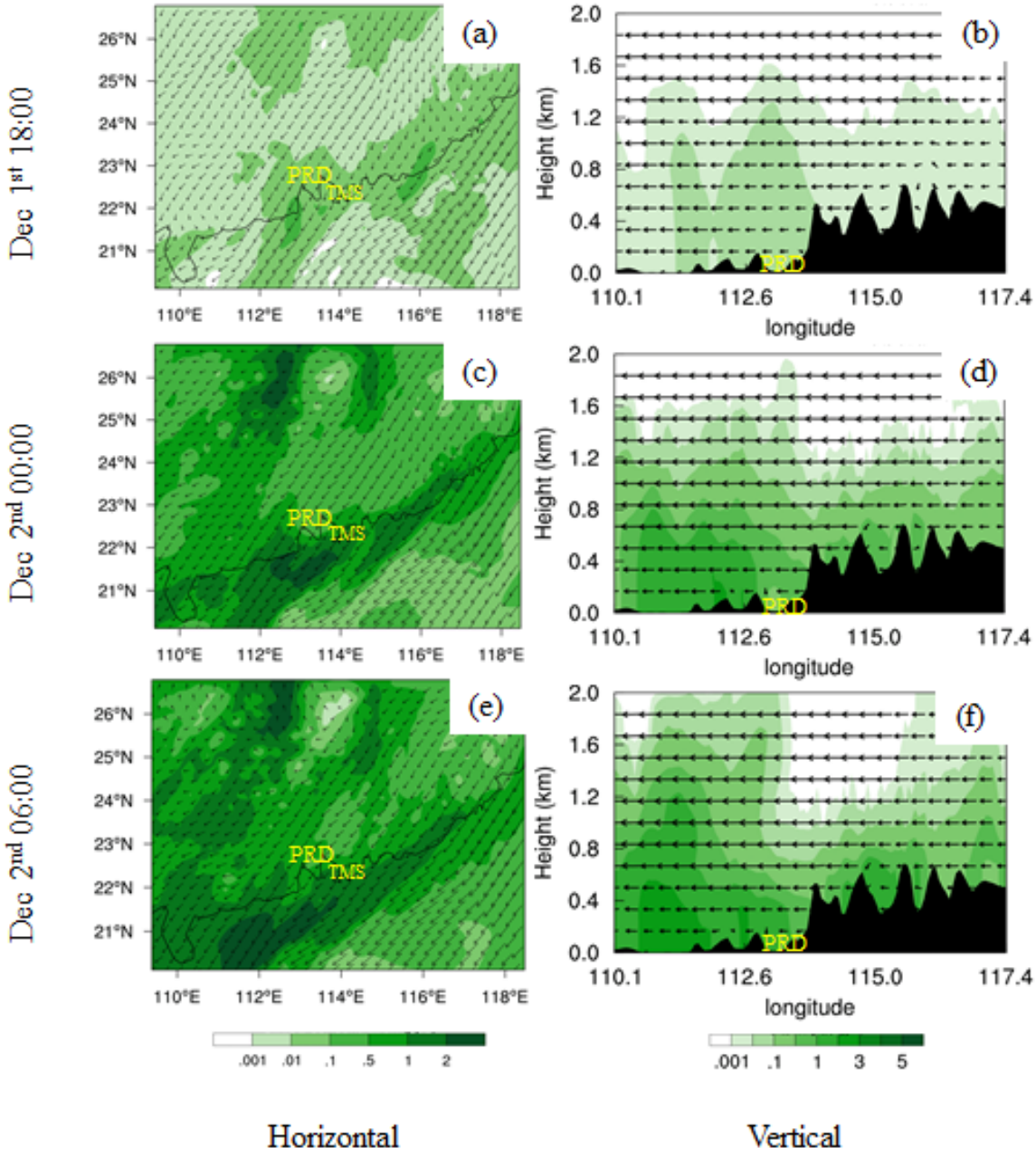

Figure 4. Horizontal distributions of $ClNO_2$ concentrations (ppb) at (a) 18:00 Dec 1, (c) 00:00 Dec 2, and (e) 06:00 Dec 2, LT within the PBL from HET+Cl case; vertical distributions of $ClNO_2$ concentrations (ppb) at (b) 18:00 Dec 1, (d) 00:00 Dec 2, and (f) 06:00 Dec 2, LT in the domain intercepting PRD and along the prevailing wind direction from HET+Cl case.

Atmos. Chem. Phys. Discuss., doi:10.5194/acp-2016-412, 2016
Manuscript under review for journal Atmos. Chem. Phys.
Published: 1 June 2016

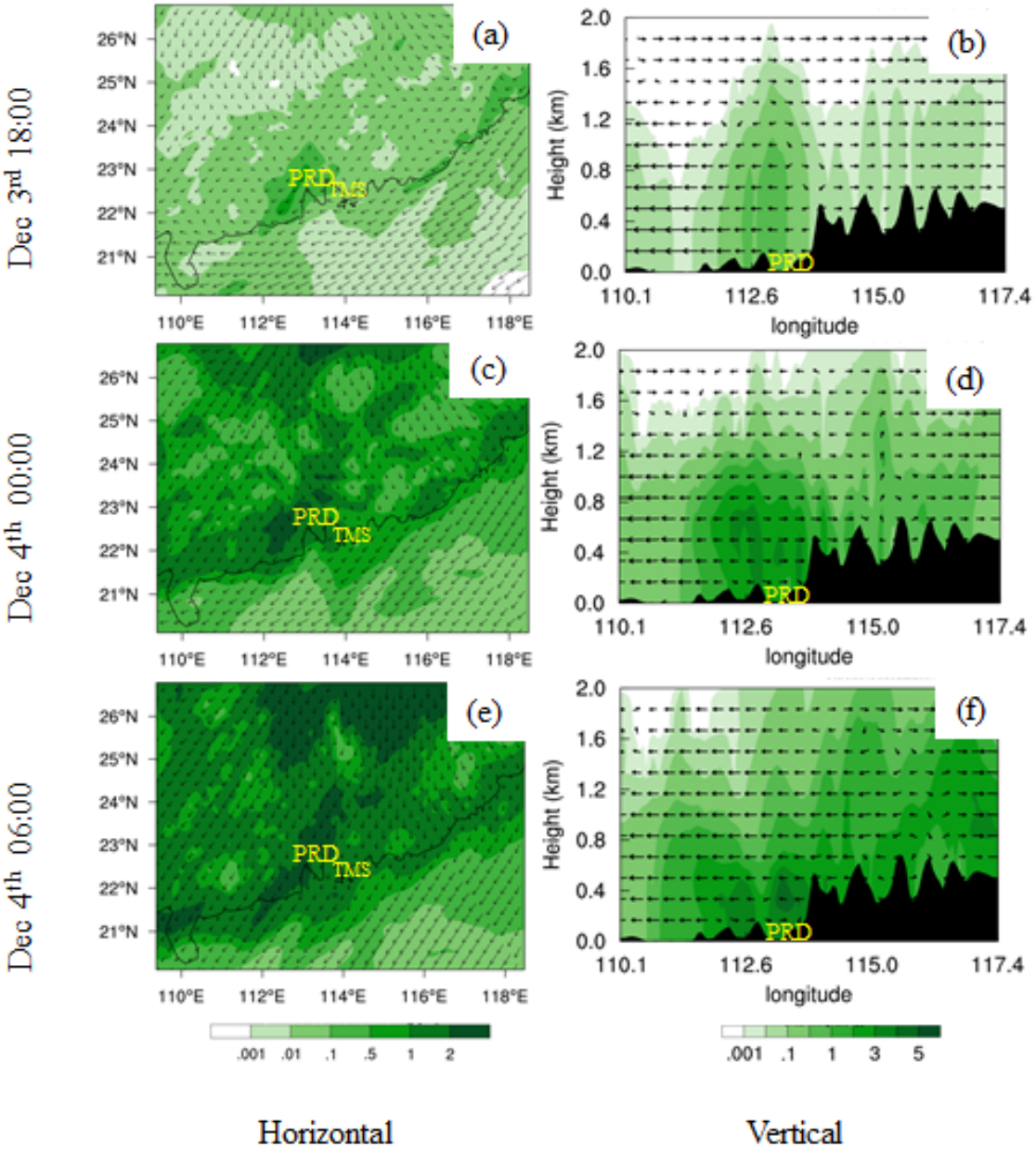

Figure 5. The same as in Figure 4, except at the night of December 3/4.

Atmos. Chem. Phys. Discuss., doi:10.5194/acp-2016-412, 2016
Manuscript under review for journal Atmos. Chem. Phys.
Published: 1 June 2016

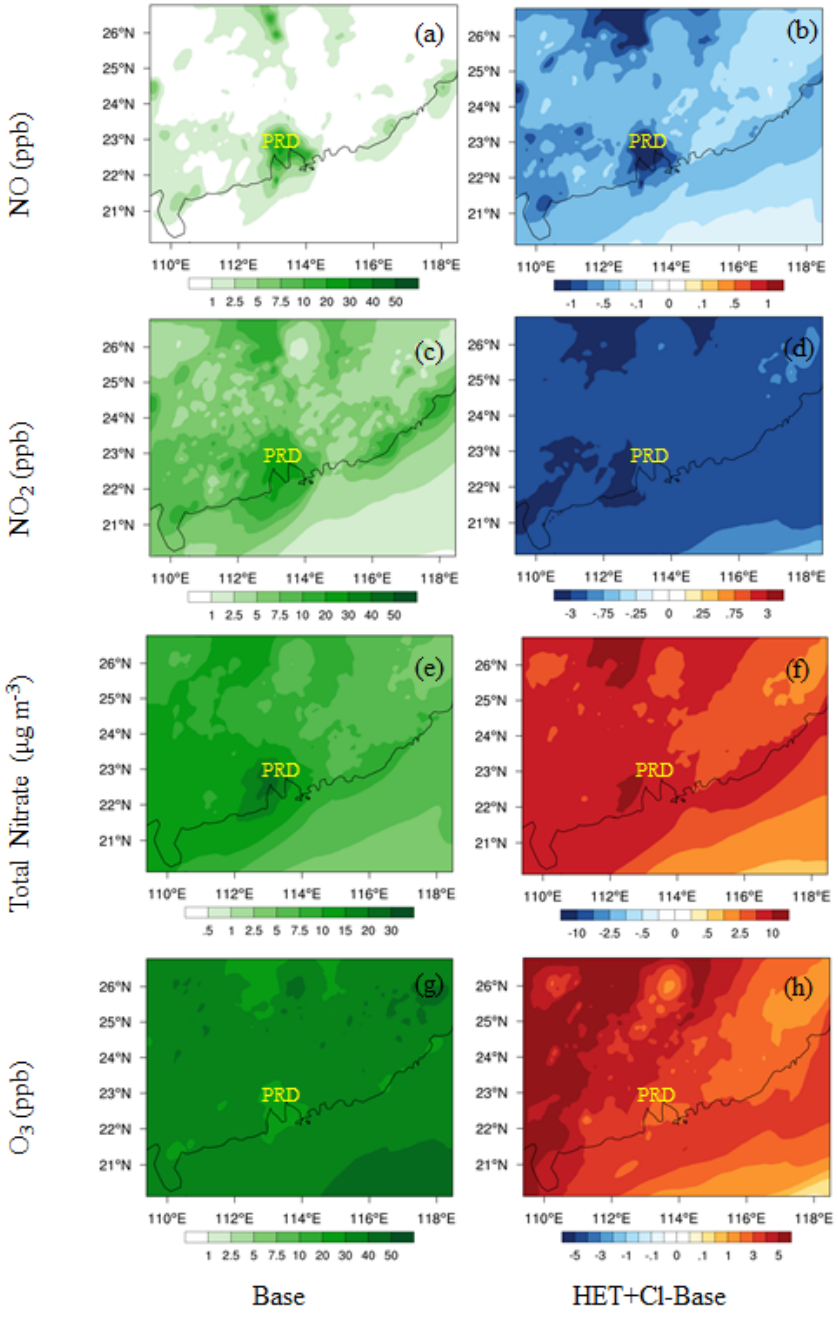

Figure 6. Horizontal distributions of (a) NO (ppb), (c) NO_2 (ppb), (e) total nitrate (μg m^{-3}) and (g) O_3 (ppb) average concentrations during the study period within the PBL from Base case; the average impacts of N_2O_5 uptake and Cl activation on (b) NO (ppb), (d) NO_2 (ppb), (f) total nitrate (μg m^{-3}) and (h) O_3 (ppb) average concentrations during the simulation period in the horizontal domain within the PBL.

Atmos. Chem. Phys. Discuss., doi:10.5194/acp-2016-412, 2016
Manuscript under review for journal Atmos. Chem. Phys.
Published: 1 June 2016

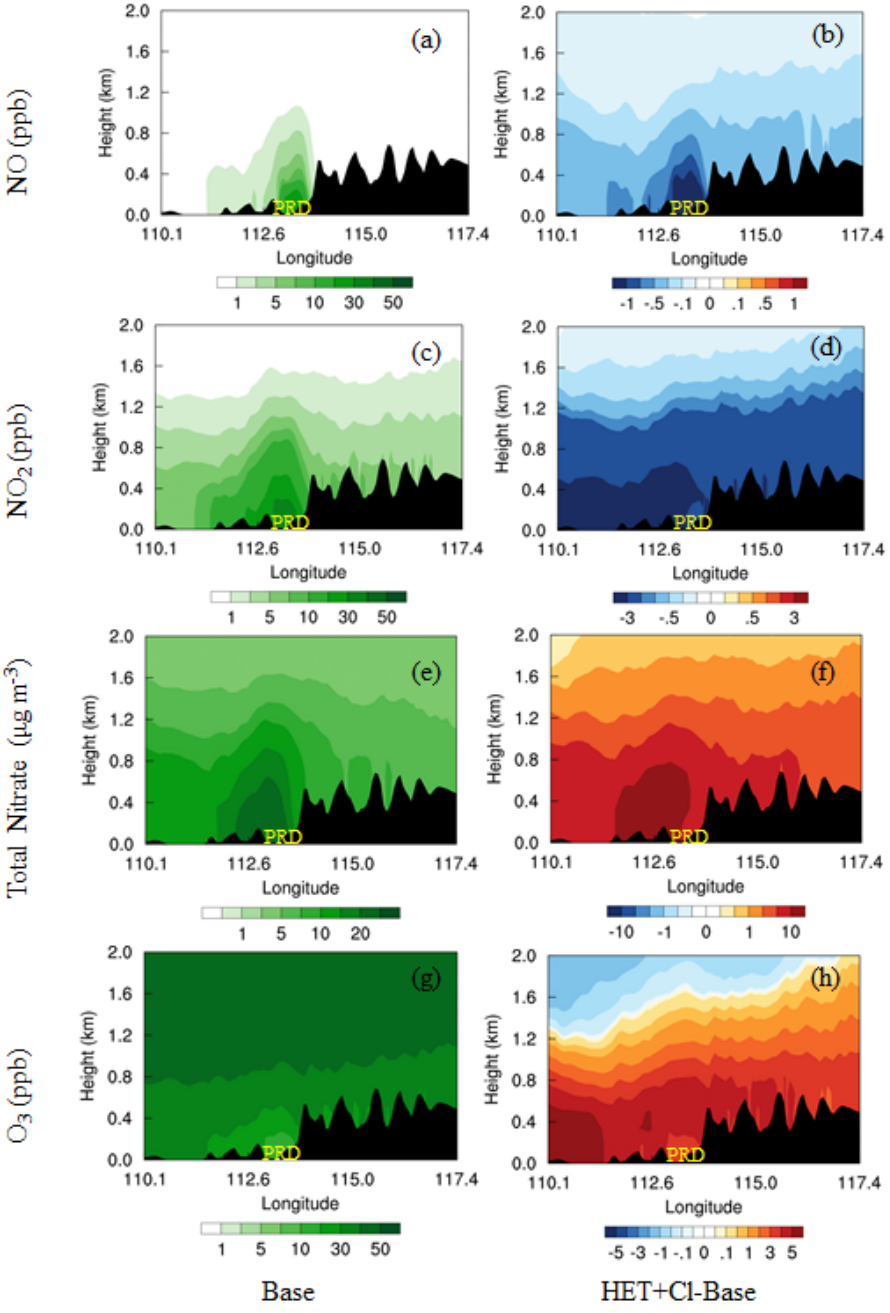

Figure 7. Vertical distributions of (a) NO (ppb), (c) NO_2 (ppb), (e) total nitrate (μg m^{-3}) and (g) O_3 (ppb) average concentrations during the study period in the domain intercepting PRD and along the prevailing wind from Base case; the average impacts of N_2O_5 uptake and Cl activation on (b) NO (ppb), (d) NO_2 (ppb), (f) total nitrate (μg m^{-3}) and (h) O_3 (ppb) average concentrations during the simulation period in the vertical domain.

Atmos. Chem. Phys. Discuss., doi:10.5194/acp-2016-412, 2016
Manuscript under review for journal Atmos. Chem. Phys.
Published: 1 June 2016

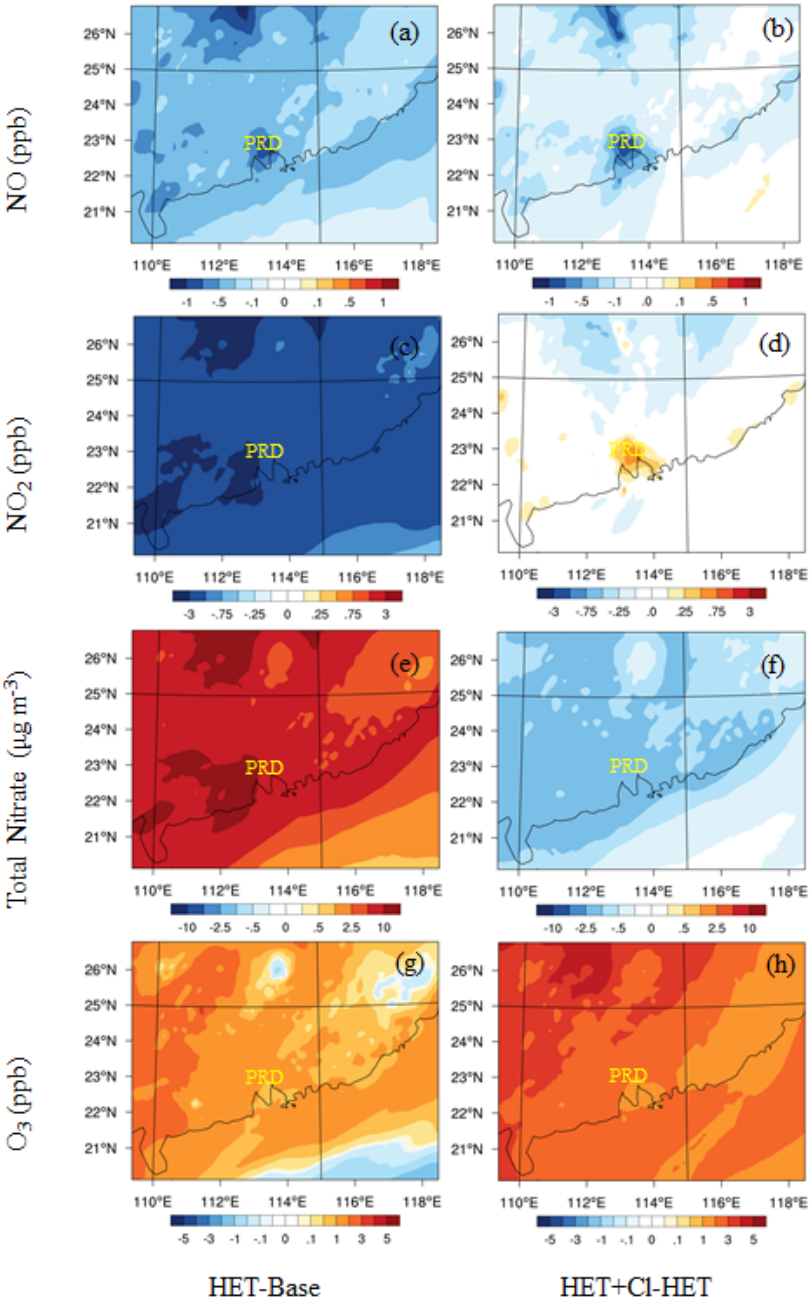

Figure 8. Average impacts of N_2O_5 heterogeneous uptake on (a) NO (ppb), (c) NO_2 (ppb), (e) total nitrate (μg m^{-3}) and (g) O_3 (ppb) average concentrations during the simulation period in the horizontal domain within the PBL; average impacts of Cl activation on (b) NO (ppb), (d) NO_2 (ppb), (f) total nitrate (μg m^{-3}) and (h) O_3 (ppb) average concentrations during the simulation period in the horizontal domain within the PBL.

Atmos. Chem. Phys. Discuss., doi:10.5194/acp-2016-412, 2016
Manuscript under review for journal Atmos. Chem. Phys.
Published: 1 June 2016

Atmospheric Chemistry and Physics Discussions

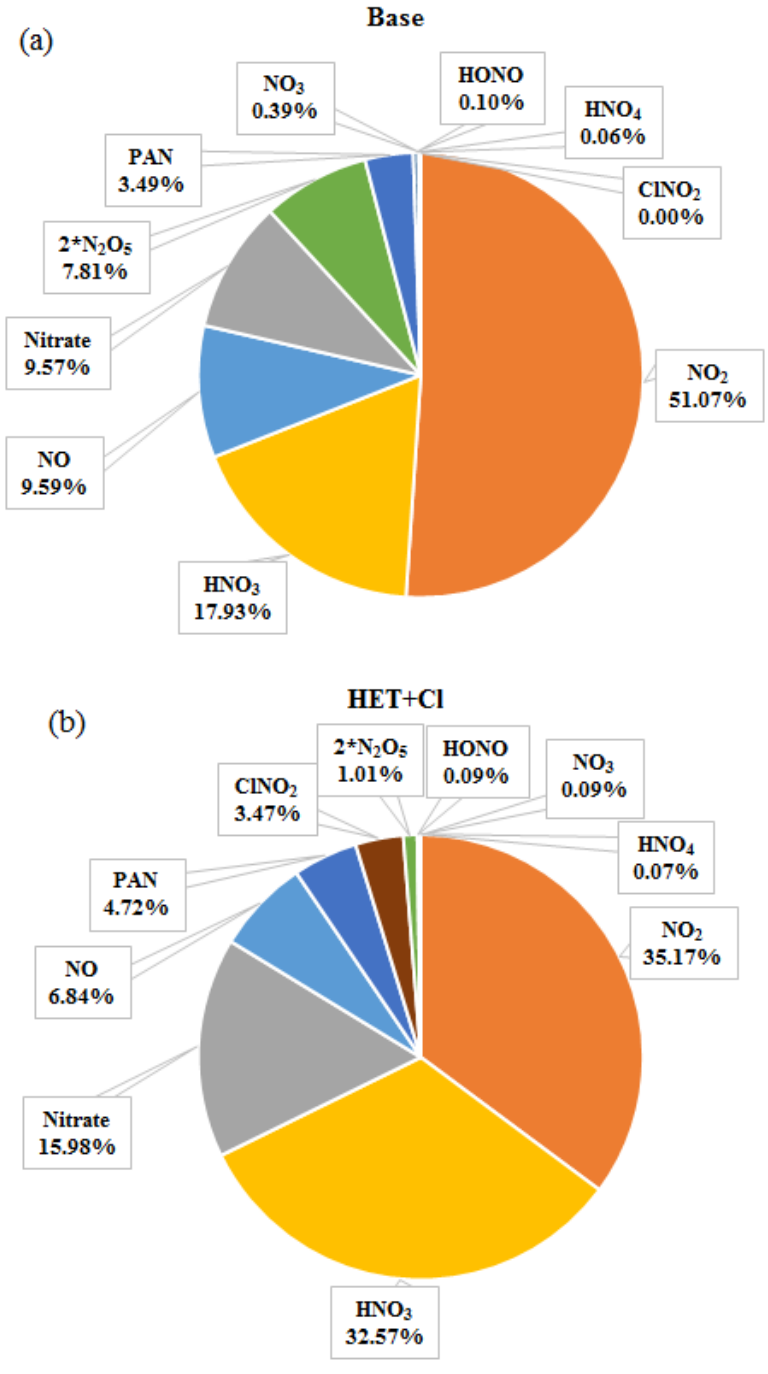

Figure 9. Average NO_y partitioning during the study period in southern China within the PBL as simulated in (a) Base and (b) HET+Cl case

Atmos. Chem. Phys. Discuss., doi:10.5194/acp-2016-412, 2016
Manuscript under review for journal Atmos. Chem. Phys.
Published: 1 June 2016

Atmospheric Chemistry and Physics Discussions

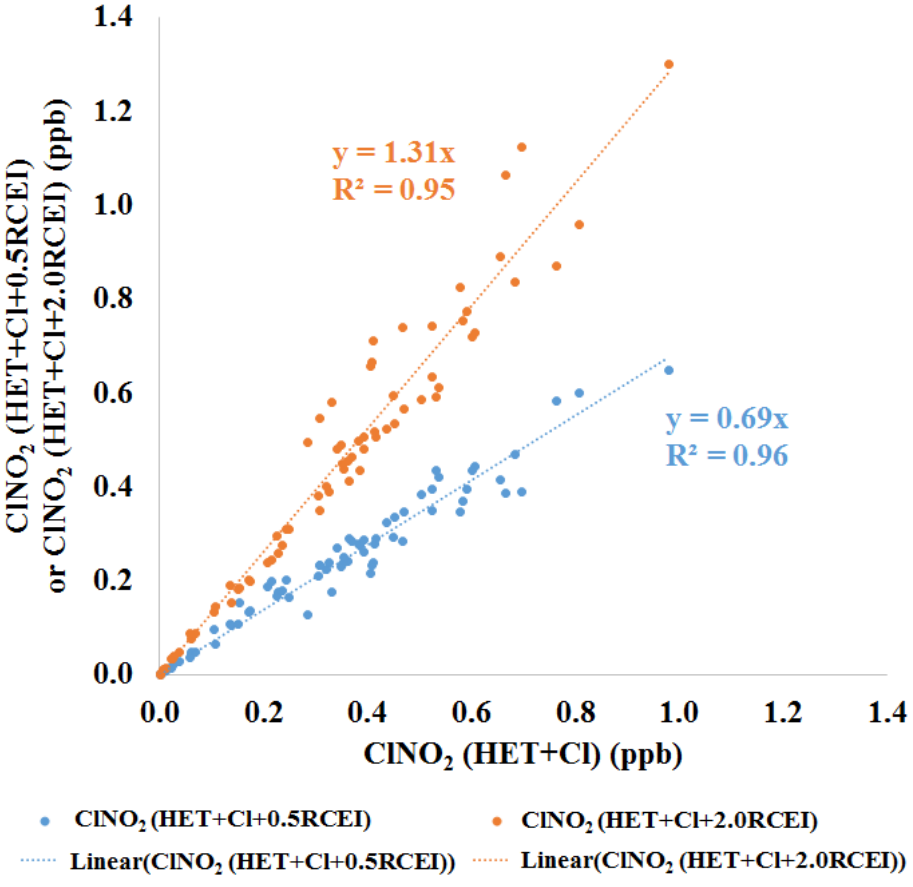

Figure 10. Scatter plots of $ClNO_2$ (ppb) from simulations with half (HET+Cl+0.5RCEI) and twice (HET+Cl+2.0RCEI) RCEI emissions against $ClNO_2$ (ppb) from simulations with original RCEI emissions (HET+Cl).

5